High-quality Si-implanted In 0.53 Ga 0.47 As epitaxial layers and their application to n + p junction devices

M. N. Blanco, E. Redondo, F. Calle, I. Mártil, and G. González-Díaz

Citation: Journal of Applied Physics **87**, 3478 (2000); doi: 10.1063/1.372369
View online: http://dx.doi.org/10.1063/1.372369
View Table of Contents: http://scitation.aip.org/content/aip/journal/jap/87/7?ver=pdfcov
Published by the AIP Publishing

High-quality Si-implanted $In_{0.53}Ga_{0.47}As$ epitaxial layers and their application to n^+p junction devices

M. N. Blanco, E. Redondo, F. Calle,[a] I. Mártil,[b] and G. González-Díaz
Departamento Electricidad y Electrónica, Fac. Físicas, Universidad Complutense, E-28040 Madrid, Spain

(Received 2 November 1999; accepted for publication 20 December 1999)

Si implantations into undoped $In_{0.53}Ga_{0.47}As$ have been carried out to obtain *n*-layers suitable for device applications. Different doses and energies have been analyzed. After rapid thermal annealing at 850–875 °C for 10–20 s, electrical activations of about 100%, and mobilities as high as 4000 $cm^2/V\,s$ were obtained. Different Hall measurements show that there is no redistribution of the dopants. Photoluminescence measurements demonstrate the satisfactory recrystallization of the lattice and the excellent activation of the dopants. Electrical characteristics of n^+p junctions made by Si implantation into Zn-doped $In_{0.53}Ga_{0.47}As$ are described. Junction behavior at forward bias could be explained by recombination in the space-charge zone mechanisms, whereas different tunneling processes dominate at reverse bias. © *2000 American Institute of Physics.* [S0021-8979(00)01807-7]

I. INTRODUCTION

$In_{0.53}Ga_{0.47}As$ in an III–V semiconductor with a high electron mobility, which makes it very attractive for high-speed logic, field-effect transistors, and microwave device applications.[1,2] The capability to absorb radiation in the wavelength range where optical fibers have minimum loss and dispersion makes $In_{0.53}Ga_{0.47}As$ very appropriate for the fabrication of planar optoelectronic integrated circuits (OEICs) on semi-insulating InP epilayers or substrates.[3,4] Both ion implantation and rapid thermal annealing (RTA) technologies in epitaxially grown InGaAs layers are very suitable for the above-mentioned applications. In particular, for a monolithic integration of a *p-i-n* photodiode (PD) and a junction field-effect transistor (JFET), Bauer *et al.*[5] reported that local Si implantations to create n^+-doped InGaAs JFET channel layer allowed the optimization of the PD and JFET devices independently.

Ion implantation of Si and Se has been used to produce *n*-type layers into $In_{0.53}Ga_{0.47}As$,[6–8] but Si is the most commonly refereed due to its low mass, which produces less lattice damage[7] and a flexible ion range. However, there are only few published reports related to the analysis of both the electrical and optical properties of *n*-type implanted layers.[9–11] Also, the available information related to the activation of implants in $In_{0.53}Ga_{0.47}As$ by RTA and its dependence with the recovery degree of the damaged lattice is difficult to find in the published literature. This fact is partially due to the inherent difficulty existing in the interpretation of the broad photoluminescence spectrum of ternary implanted semiconductor compounds.[12,13] On the other hand, there are several reports on *p-n* junctions made on *n*-type $In_{0.53}Ga_{0.47}As$ substrates,[14,15] but not too much research has been done about diodes over *p*-type epilayers.[16] In particular, it is necessary to study the relationship of their current–voltage characteristics with the properties of the *n*-type implanted layers used to fabricate the mentioned devices.

The aim of this article is to study the electrical and optical characteristics of Si-implanted $In_{0.53}Ga_{0.47}As$ to obtain *n*-type layers suitable for device applications. We analyzed a huge range of implantation energies and doses, and different rapid thermal annealing cycles for the activation of the dopants. Hall measurements and photoluminescence (PL) characterization of the samples are made to confirm the lattice recovery of the implanted layers after the high RTA treatment. Finally, the present work is focused on examining the effects of implantation and annealing parameters on the current–voltage characteristics of the n^+p junctions in $In_{0.53}Ga_{0.47}As$ made by the Si-implanted layers previously analyzed.

II. EXPERIMENT

Unintentionally doped $In_{0.53}Ga_{0.47}As$ epilayers supplied by EPI[17] were grown lattice matched to (100) InP:Fe substrates by metalorganic vapor phase epitaxy (MOVPE). The layers were 1.9 μm thick with a net donor concentration of $5\times10^{14}\,cm^{-3}$.

N-type layers were obtained by Si implantation at room temperature, with different energies (from 50 to 225 keV) and doses (from 1×10^{13} to $5\times10^{14}\,cm^{-2}$). All the implantations were performed with the samples tilted 7° out of the ion beam direction, to minimize channeling. The activation of the dopants were done by RTA in a MPT reactor, using a graphite susceptor in a P-rich atmosphere, with the samples sandwiched between two Si wafers in the so-called proximity geometry. The RTA cycles were performed at temperatures of 850 and 875 °C during 10 or 20 s.[18]

Contacts for electrical measurements were done by evaporating AuGe:Au dots, and a posterior alloying treatment at 420 °C during 1 min in Ar ambient. Electrical acti-

[a]Also at Departamento de Ingeniería Electrónica, ETSI Telecomunicaciones, Universidad Politécnica, 28040 Madrid, Spain.
[b]Author to whom correspondence should be addressed; electronic mail: imartil@eucmax.sim.ucm.es

vation and Hall mobility values of cross-patterned samples were obtained by the Van der Pauw method, with a system equipped with high impedance Keithley electrometers for voltage measurements and a Keithley 220 current source. The scattering factor was kept equal to 1 in all cases. The ternary semiconductor material out of the cross pattern was etched to minimize possible shunt conduction paths that could affect the measurements. Activation values were not corrected to account for surface depletion, which would increase the percentage of apparent activated dopants. The electrical profile of the implanted Si dopants was measured by the differential Hall technique, using an etching solution of H_3PO_4:H_2O_2:$38H_2O$, which has an etch rate of about 200 Å/min.

Low-temperature photoluminescence (PL) was performed using a He–Ne laser at 632.8 nm, with 1.5 mW of incident power, a Jobin-Yvon H-25 monochromator and a liquid nitrogen cooled Ge detector, using lock-in techniques.

n^+-p junctions were done over Zn-doped $In_{0.53}Ga_{0.47}As$ epilayers ($p \approx 1\times10^{16}\,cm^{-3}$) using the implantation and annealing procedures described above. Two different devices were analyzed: one of them was obtained with a single Si implantation at 150 keV with $1\times10^{14}\,cm^{-2}$, and the other with a dual Si implantation at 50/225 keV with $2\times10^{14}/1\times10^{13}\,cm^{-2}$. Ohmic contacts for the n^+ and p layers were AuGe/Au and AuZn/Au, respectively. They were obtained by thermal evaporation, after an alloying cycle at 420 °C for 1 min. Mesa devices with different areas were defined by usual photolithographic methods on the n^+-type layer, and subsequently isolated by wet etching. Current–voltage characteristics were measured using a Keithley 230 V source, a Keithley 182 sensitive digital voltmeter, and a Keithley 2001 precision multimeter for current measurements. Both forward and reverse characterizations were done at variable temperature, in the range of 190–320 K.

III. RESULTS AND DISCUSSION

A. Si-implanted $In_{0.53}Ga_{0.47}As$ layers

Hall measurements reveal that $In_{0.53}Ga_{0.47}As$ layers implanted at high Si doses ($>1\times10^{14}\,cm^{-2}$) show electrical activation and Hall mobility values that are not too much dependent on the annealing time. This behavior is due to different factors. For these doses (from 1×10^{14} to $5\times10^{14}\,cm^{-2}$), the amorphization limit has been reached, so it is not possible to recover the lattice damage even after an annealing at high temperatures for long times. On the other hand, the net electron concentration is high enough ($\sim 2\times10^{18}$–$2\times10^{19}\,cm^{-3}$), so that the dispersion mechanism through impurities is dominant. Thus, the reduction of lattice defects by means of longer annealing times is not relevant and has no influence on the mobility, which remains almost constant with the annealing time. For low doses, it should be noted that the electrical activation of these annealed layers does not exhibit any clear dependence on the anneal time.

The effect of the annealing temperature is shown in Fig. 1, for Si-implanted layers with a dose of $5\times10^{13}\,cm^{-2}$, after a RTA during 10 s. It is seen that higher annealing temperatures result in better electrical activations and electron mobilities, independently of implant energy. Also, rapid thermal annealings at temperatures higher than 875 °C resulted in a strong degradation of the semiconductor surface. So, the optimum annealing cycle for Si implants into $In_{0.53}Ga_{0.47}As$ is at 875 °C during 10 or 20 s.

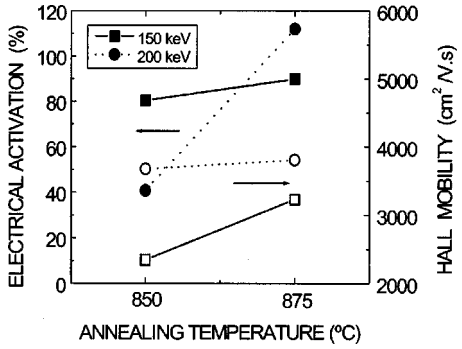

FIG. 1. Effect of the annealing temperature over the electrical activation and Hall mobility of Si-implanted $In_{0.53}Ga_{0.47}As$ layers with a dose of $5\times10^{13}\,cm^{-2}$ for different implantation energies. The annealing time was kept constant at 10 s.

The effect of the dose on the electrical activation of implanted layers was investigated for two different annealing temperatures, at an implantation energy of 150 keV, as shown in Fig. 2. The electrical activation is about 90% for the intermediate doses, decreasing for both lower and higher doses. The reduction in activation for the highest doses is usually explained by the amphoteric nature of Si in $In_{0.53}Ga_{0.47}As$, the stoichiometric disturbances produced in the crystal lattice,[19,20] and the significant implantation damage oriented at these doses. However, as shown in Fig. 2, the maximum electrical activation obtained for $5\times10^{14}\,cm^{-2}$ Si implants is about 60%, the highest value ever refereed in the literature for comparable Si implants doses in non intentionally doped $In_{0.53}Ga_{0.47}As$ epitaxial layers. On the other hand, the inferior electrical activation values obtained for lower doses (up to 70%) in comparison with medium doses (up to 90%) could be attributed to different factors: carrier surface depletion[21] and shunt conductance by the substrate. As previously described, the $In_{0.53}Ga_{0.47}As$ epilayers used in this work have a net donor concentration in the order of 5

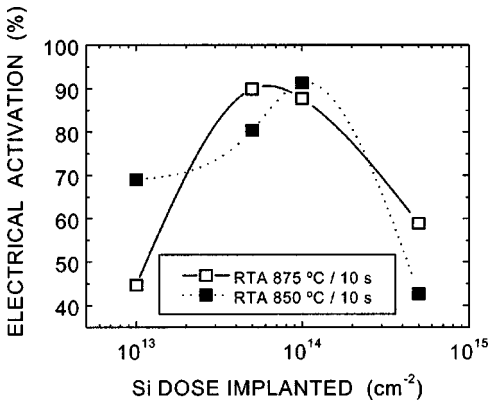

FIG. 2. Variation of electrical activation with implant dose for 150 keV Si implants in undoped $In_{0.53}Ga_{0.47}As$, activated by RTA at 850 and 875 °C during 10 s.

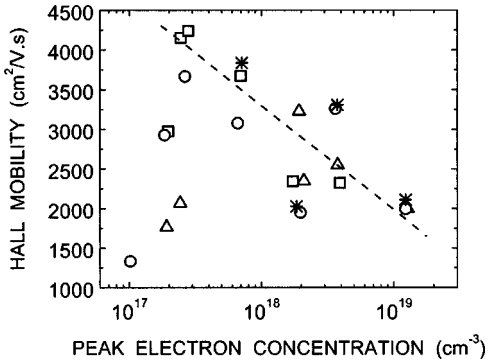

FIG. 3. Hall mobility of Si-implanted $In_{0.53}Ga_{0.47}As$ as a function of peak electron concentration, for different implant energies and annealing cycles [850 °C/10 s (□), 875 °C/5 s (○), 875 °C/10 s (△), 875 °C/20 s (*)]. Peak electron concentration takes into account the measured electrical activation. The dashed line is a guide for the eye.

$\times 10^{14}\,cm^{-3}$. Because of that, Hall measurements of the implanted layers could be influenced by the shunt conductance in the nonimplanted $In_{0.53}Ga_{0.47}As$ layer. This effect is stronger at lower doses, that is, lower electron concentrations.

Figure 3 shows Hall mobility values as a function of the peak electron concentration for the different implantation processes and annealing cycles analyzed. Peak electron concentrations are obtained by theoretical SRIM-96 profiles modified by the measured electrical activation. The general behavior of mobility measurements is in reasonable agreement with calculations by Takeda[22] on comparably doped InGaAs. The high values of mobility obtained (~4250–3000 $cm^2/V\,s$) for medium and high doses indicate a proper crystalline recovery of the lattice after annealing. At low doses, peak electron concentration around $2\times 10^{17}\,cm^{-3}$, there is a considerable dispersion of the measured Hall mobility values, from 1500 to 3000 $cm^2/V\,s$, as displayed in Fig. 3. This behavior could be attributed to the different compensation ratios in the implanted layers. In fact, calculated electron Hall mobilities in $In_{0.53}Ga_{0.47}As$ layers with a net electron concentration of about $2\times 10^{17}\,cm^{-3}$, lie between 2000 and 7000 $cm^2/V\,s$ for carrier compensation ratios from 1 to 10,[22] in good agreement with the data observed in our samples.

Figure 4 shows the carrier concentration and Hall mobility depth profile for a sample implanted at 150 keV with a dose of $1\times 10^{14}\,cm^{-2}$, after a RTA at 875 °C for 10 s. It can be seen that the measured carrier concentration profile perfectly fits the SRIM-96 theoretical Si-implanted profile, showing that no redistribution of the dopants occurred during RTA treatment. Hall mobility also shows good values over the whole implanted region. Therefore, the electrical characterization of Si implants at 150 keV with $1\times 10^{14}\,cm^{-2}$, annealed at 875 °C for 10 s, suggests that these *n* layers are appropriate for *p-n* junction devices, as shown in the next section.

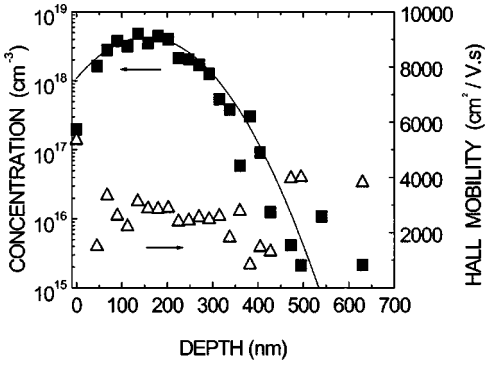

FIG. 4. Electron concentration and Hall mobility depth profiles obtained by differential Hall measurements for Si implants at 150 keV with dose of $1\times 10^{14}\,cm^{-2}$, after 875 °C/10 s RTA. SRIM-96 theoretical profile (—) is also shown for comparison.

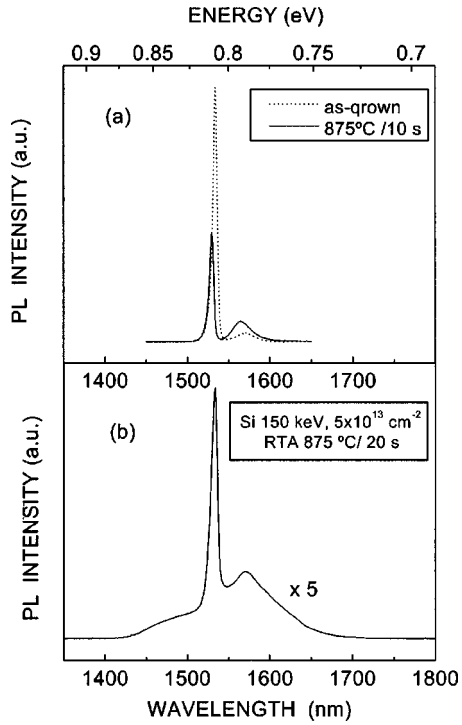

FIG. 5. PL spectrum (14 K, 1.5 mW) of: (a) undimmed $In_{0.53}Ga_{0.47}As$ as-grown and rapid thermal annealed (875 °C/10 s); (b) Si implanted ($5\times 10^{13}\,cm^{-2}$, 150 keV) after a RTA at 875 °C/20 s. The same scales of vertical axis are used in (a) and (b).

The PL spectrum of as-grown nonimplanted $In_{0.53}Ga_{0.47}As$ is shown in Fig. 5(a). It presents a dominant emission at 1534 nm (0.808 eV) due to the superposition of several elementary near-band-gap recombination mechanisms [excitons bound to donor impurities, donor to valence band recombinations ($D-V$), etc.]; and a broader band at 1570 nm (0.790 eV) due to donor-acceptor ($D-A$) pair recombination, in agreement with the assignment of the 0.79 eV band reported by Chen and Kim.[23] The spectrum of a sample annealed at 875 °C during 10 s is shown in the same figure. It also presents two transitions, at 1530 nm (0.810 eV) and 1565 nm (0.792 eV), respectively. Because the relative separation between them is the same than in the nonannealed material (18 meV), we conclude that both transitions have the same origin as in the as-grown sample, that is, $D-V$ transition at 1530 nm and $D-A$ recombination at 1565 nm. The energy displacement of 2 meV could be explained by composition fluctuations in the order of 0.2%, as previously reported results reveal.[24,25] The intensification of $D-A$ peak in annealed samples is probably due to the outdiffusion

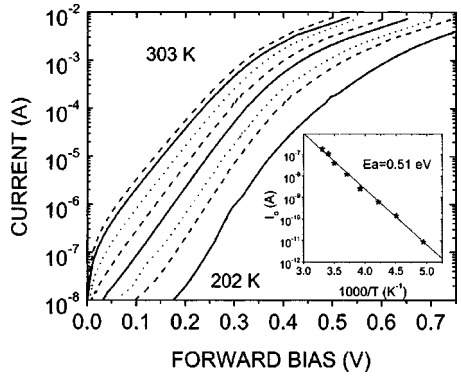

FIG. 6. Forward characteristics as a function of temperature (303, 294, 286, 271, 255, 237, 222, and 202 K) for a *p-n* junction made by Si implantation ($1\times10^{14}\,cm^{-2}$, 150 keV) into $In_{0.53}Ga_{0.47}As$:Zn after a RTA at 875 °C for 10 s. The Arrhenius plot of the reverse saturation current is shown as an inset.

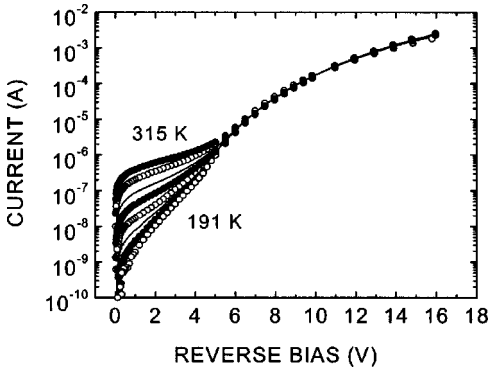

FIG. 7. Reverse characteristics as a function of temperature (315, 303, 288, 273, 251, 231, 211, and 191 K) for a junction made by a dual Si implantation ($2\times10^{14}\,cm^{-2}$/50 keV and $1\times10^{13}\,cm^{-2}$/225 keV) into $In_{0.53}Ga_{0.47}As$:Zn after a RTA at 875 °C for 20 s.

of a residual impurity to the surface during the RTA treatment, as obtained in InP.[26]

The PL spectrum of Si-implanted $In_{0.53}Ga_{0.47}As$ ($5\times10^{13}\,cm^{-2}$, 150 keV), after a RTA at 875 °C for 20 s, is shown in Fig. 5(b). The high PL intensity measured in these samples shows that the annealing treatment decreases the concentration of nonradiative damage-related centers in the implanted material, reflecting the adequate recovery of the bombarded lattice. The spectrum is similar to those of as-grown and annealed undoped samples. However, there is a small shoulder at high energies, probably ascribed to the filling of the conduction-band states. This effect has been previously reported in highly III–V semiconductors, either grown[27] or implanted,[28] and reflects the successful activation of the Si impurities by the RTA process.

B. Implanted InGaAs *p-n* junctions

Two different *p-n* junctions over *p*-$In_{0.53}Ga_{0.47}As$ substrates have been analyzed. The first one has been formed with a single Si implantation at high dose ($1\times10^{14}\,cm^{-2}$) and low energy (80 keV), that is, the doping parameters employed for ohmic contacts. The *n* zone of the second junction is appropriate to obtain the channel region of field effect transistor devices, i.e., low dose ($1\times10^{13}\,cm^{-2}$) and high energy (225 keV). At this last case, an additional superficial and highly doped Si implantation is also needed to obtain good quality ohmic contacts. These *p-n* devices are called dual implanted junctions.

1. Single implants

Figure 6 presents the forward bias $I-V$ characteristics of an $In_{0.53}Ga_{0.47}As$:Zn n^+p junction at different temperatures of measurement. The *n* region was made by $1\times10^{14}\,cm^{-2}$ Si implantation at 150 keV, after a RTA at 875 °C for 10 s, i.e., in the same conditions as used for undoped samples. It can be seen that this device shows moderate values of series resistance, and there is no evidence of shunt resistance. Ideality factor values increase with decreasing temperature from 1.34 at 303 K to 1.52 at 202 K. The reverse saturation current is thermally activated, with an activation energy of 0.51 eV, as shown in the inset of Fig. 6. These facts lead to the conclusion that the dominant conduction mechanism at forward bias is the recombination in the space charge zone. A more detailed discussion concerning this behavior can be found in Ref. 16.

2. Dual implants

p-n junctions made by a double Si implantation ($1\times10^{13}\,cm^{-2}$ at 225 keV and $2\times10^{14}\,cm^{-2}$ at 50 keV) into $In_{0.53}Ga_{0.47}As$:Zn were also analyzed. The implants at lower energy and high dose were necessary to obtain good quality ohmic contacts. The forward characteristics were similar to those obtained for single implanted *p-n* junctions, independently of the annealing time. The temperature dependence of the saturation current yields an activation energy for the reverse current, I_0, of 0.53 eV, and the conduction mechanism was also dominated by recombination in the space-charge zone.

The reverse $I-V$ characteristics at different temperatures for a dual Si-implanted *p-n* junction, after an annealing treatment at 875 °C for 20 s, is shown in Fig. 7. The weak temperature dependence of the reverse $I-V$ characteristics is indicative of tunneling conduction. As we demonstrated in a previous paper,[16] reverse characteristics in Si-implanted $In_{0.53}Ga_{0.47}As$:Zn were successfully simulated by different tunneling mechanisms. $I-V$ experimental curve at low bias was explained by thermally assisted tunneling through a trap with an activation energy of 0.21 eV. On the other hand, medium and high reverse bias characteristics were both perfectly fitted to defect assisted tunneling processes, via energy states at 0.13 and 0.70 eV, respectively. Similar reverse $I-V$ curves were recently reported on GaInSb photodetectors,[29] although no association of the $I-V$ reverse behavior to any particular conduction mechanism was discussed. Probably, thermally and defect assisted tunneling processes could explain their characteristics at reverse bias.

The reverse characteristics of these junctions show a clearer dependence on the annealing time or the use of additional Si implantations than the forward characteristics. It is just deduced from Fig. 8, where the effects of implantation dose and annealing time on the reverse $I-V$ curves are displayed. As it can be seen, the effect of Si dose is to increase

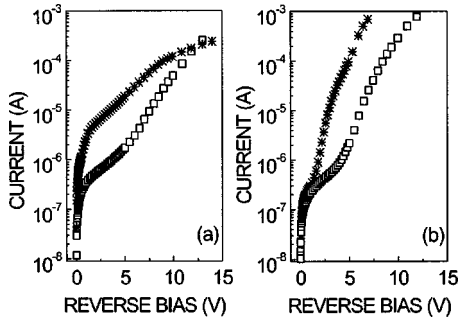

FIG. 8. (a) Effect of Si dose [(□) $1\times10^{13}\,cm^{-2}$, (*) $1\times10^{14}\,cm^{-2}$], on the reverse characteristics of *p-n* junctions made by Si implantations into $In_{0.53}Ga_{0.47}As$:Zn after a RTA at 875 °C for 20 s. (b) Effect of annealing time [(*) 10 s, (□) 20 s] on the reverse characteristics of *p-n* junctions made by Si implantation into $In_{0.53}Ga_{0.47}As$:Zn after a RTA at 875 °C.

the reverse conduction, while the use of longer annealing times decreased the reverse current. This behavior was previously observed by Martin *et al.* in Si-implanted InP junctions[30] and was explained in terms of the relation of the reverse current with the trap concentration.

IV. CONCLUSIONS

High quality Si-implanted $In_{0.53}Ga_{0.47}As$ layers have been analyzed. After a rapid thermal annealing at 850–875 °C for 10–20 s, the samples exhibit electrical activations higher than 100% and Hall mobilities in the range of 2000–4000 $cm^2/V\,s$. The electrical depth profile shows that there is not redistribution of impurities after RTA, even after implantation at high doses. Photoluminescence measurements show a good recovery of the lattice damage. A small shoulder at high-energy reflects the successful activation of the dopants.

Electrical characteristics of *p-n* junctions made by Si implantations in $In_{0.53}Ga_{0.47}As$:Zn have been reported. Forward $I-V$ curves could be explained by recombination mechanisms at the space-charge zone, while reverse characteristics were successfully modeled by taking into account different tunneling processes: a thermally assisted tunneling at low bias, and defect assisted tunneling both at medium and high bias. On the other hand, Si-implanted dose and annealing time significantly affect the reverse conduction.

ACKNOWLEDGMENTS

The authors would like to thank CAI de Implantación Iónica from the Complutense University in Madrid for assistance with ion implantation. This work was partially supported by the Spanish CICYT under Grant No. TIC 98/0740.

[1] L. Y. Leu, J. T. Gardner, and S. R. Forrest, J. Appl. Phys. **69**, 1052 (1991).
[2] A. Ouacha, M. Wilander, R. Plana, J. Graffeuil, and L. Escotte, Appl. Phys. Lett. **78**, 2565 (1995).
[3] Y. G. Wey, D. L. Crawford, K. Giboney, J. E. Bowers, M. J. Rodwell, P. Silvestre, M. J. Hafich, and G. Y. Robinson, Appl. Phys. Lett. **58**, 2156 (1991).
[4] D. S. Kim, S. R. Forrest, M. J. Lange, G. H. Olsen, and W. Kosonocky, IEEE Photonics Technol. Lett. **8**, 566 (1996).
[5] J. G. Bauer, H. Albbrecht, L. Hoffmann, D. Römer, and J. W. Walter, IEEE Photonics Technol. Lett. **4**, 253 (1992).
[6] M. V. Rao, S. M. Gulwadi, P. E. Thompson, A. Fathimulla, and O. A. Aina, J. Electron. Mater. **18**, 131 (1989).
[7] T. Penna, B. Tell, A. S. H. Liao, T. J. Bridges, and G. Burkhardt, J. Appl. Phys. **57**, 351 (1985).
[8] B. J. Sealy, M. A. Shahid, M. Anjum, S. S. Gill, and J. H. Marsh, Nucl. Instrum. Methods Phys. Res. B **7**, 423 (1985).
[9] M. V. Rao and W. Kruppa, Electron. Lett. **22**, 299 (1986).
[10] E. Hailemariam, S. J. Pearton, W. S. Hobson, H. S. Luftman, and A. P. Perley, J. Appl. Phys. **71**, 215 (1992).
[11] S. G. Liu, S. Y. Narayan, C. W. Magee, C. P. Wu, F. Kolondra, J. P. Paczkowski, and D. R. Capewell, Mater. Res. Soc. Symp. Proc. **92**, 375 (1987).
[12] M. Maier and J. Selders, J. Appl. Phys. **60**, 2783 (1986).
[13] S. J. Pearton, W. S. Hobson, A. P. Kinsella, J. Kovalchick, U. K. Chakrabarti, and C. R. Abernathy, Appl. Phys. Lett. **56**, 1263 (1990).
[14] B. Tell, R. F. Leheny, A. S. H. Liao, T. J. Bridges, E. G. Burkhardt, T. Y. Chang, and E. D. Beebe, Appl. Phys. Lett. **44**, 438 (1984).
[15] A. Zemel, B. Tell, R. F. Leheny, T. Harrison, T. J. Bridges, E. G. Burkhardt, A. S. H. Laio, and E. D. Beebe, J. Appl. Phys. **56**, 1856 (1984).
[16] M. N. Blanco, E. Redondo, C. León, J. Santamaría, and G. González-Díaz, Nucl. Instrum. Methods Phys. Res. B **147**, 166 (1999).
[17] Epitaxial Products International Ltd., Cypress Drive, St. Mellons, Cardiff, CF3 0EG, UK.
[18] M. N. Blanco, E. Redondo, C. León, J. Santamaría, and G. González-Díaz, J. Mater. Sci.: Mater. Electron. **10**, 425 (1999).
[19] W. Lee and C. G. Fonstad, J. Appl. Phys. **61**, 5272 (1987).
[20] M. V. Rao, S. M. Gulwadi, P. E. Thompson, A. Fathimulla, and O. A. Aina, J. Electron. Mater. **18**, 131 (1989).
[21] A. Chandra, C. E. C. Wood, D. W. Wooddard, and L. F. Eastman, Solid-State Electron. **22**, 645 (1979).
[22] Y. Takeda, in *GaInAsP Alloy Semiconductors*, edited by T. P. Pearsall (Wiley, New York, 1982), Chap. 9, p. 227.
[23] Y.-S. Chen and O. Kim, J. Appl. Phys. **52**, 7392 (1981).
[24] A. F. S. Penna, J. Shah, A. E. DiGiovanni, and A. G. Dentai, Solid State Commun. **51**, 217 (1984).
[25] A. F. S. Penna, J. Shah, T. Y. Chang, M. S. Burroughs, R. E. Nahory, M. Tamargo, and H. M. Cox, Solid State Commun. **51**, 425 (1984).
[26] P. K. Bhattacharya, W. H. Goodman, and M. V. Rao, J. Appl. Phys. **55**, 509 (1984).
[27] Y. K. Su, M. C. Wu, C. H. Huang, and B. S. Chiu, J. Appl. Phys. **64**, 2211 (1988).
[28] D. J. Olego and H. B. Serreze, J. Appl. Phys. **58**, 1979 (1985).
[29] H. X. Yuan, D. Grubisic, and T. T. S. Wong, J. Electron. Mater. **28**, 39 (1999).
[30] J. M. Martin, S. Garcia, I. Mártil, G. González-Díaz, E. Castán, and S. Dueñas, J. Appl. Phys. **78**, 5325 (1995).